The Novel Ferroptosis-related Gene Markers That Can Predict the Survival in Gastric Cancer Patients

Bang Chen
Department of General Surgery, First Affiliated Hospital of Anhui Medical University
https://orcid.org/0000-0002-3068-7064
Xin Xu
Department of General Surgery, The First Affiliated Hospital of Anhui Medical University
ShaoFu Zhu
Department of General Surgery, The First Affiliated Hospital of Anhui Medical University
ShiYi Yang
Department of General Surgery, The First Affiliated Hospital of Anhui Medical University
Kang Yang
Department of General Surgery, The First Affiliated Hospital of Anhui Medical University
MengYao Jin
The First Clinical College, Anhui Medical University
Tianbin Wang
Department of General Surgery, The First Affiliated Hospital of Anhui Medical University
Tao Men
Department of General Surgery, The First Affiliated Hospital of Anhui Medical University
Guodong Cao
Department of General Surgery, The Affiliated Hospital of Anhui Medical University
Bo Chen (chenbo831116@163.com)
Department of General Surgery, the First Affiliated Hospital of Anhui Medical University, Aahui, China.
https://orcid.org/0000-0003-0524-1105

Research

Keywords: Gastric cancer, Ferroptosis, DEGs, Tumor Immunology, Extracellular matrix

Posted Date: November 20th, 2020

DOI: https://doi.org/10.21203/rs.3.rs-111305/v1

Abstract

Background: Gastric cancer(GC) refers to malignant tumor that derived from gastric epithelial cells. Ferroptosis is another programmed cell demise mode that is Fe-dependent, unique concerning apoptosis, cell necrosis, and autophagy. Current research demonstrates that ferroptosis assumes a basic part of cancer biology. Extracellular matrix(ECM) has been confirmed to play an essential role in the proliferation, apoptosis, metabolism and differentiation of tumor cells. As an important component of the tumor microenvironment, ECM interacts with the immune microenvironment and affects tumor development and progression.

Methods: GC data were downloaded from the TCGA database. Furthermore, 259 ferroptosis-related genes were acquired with the FerrDb database. COX regression analysis was used to screen ferroptosis-related genes related to GC's prognosis, and these genes constructed the prediction model. The risk score of the model and clinical data of GC were further analyzed to get the correlation between the model and the overall survival(OS) rate and clinicopathological features. Finally, GO and KEGG enrichment analysis was carried out on the genes of the model. To further analyze the correlation between the genes in the model and tumor immunity, ssGSEA was used to score immune cells and calculate immune-related pathways' activity quantitatively.

Results: A prognosis model was constructed according to the 11 ferroptosis-related genes related to prognosis to predict the prognosis of GC patients better. According to univariate and multivariate, risk score can be regarded as an independent predictor.

Conclusions: we identified 11 ferroptosis-related genes (NOX4, NOX5, SLC1A5, GLS2, MYB, TGFBR1, NF2, ZFP36, DUSP1, SLC1A4, SP1), which affected the prognosis of GC patients.

Background

Gastric disease (GC) is a regular malignant tumor beginning starting with the gastric mucosal epithelium. Worldwide, GC's incidence is at the forefront of all cancers, with the second-highest mortality rate[1]. Due to differences in China's dietary structure and lifestyle, GC is the second most common cancer in China and has a high mortality rate[2]. At present, more and more studies construct disease prediction models by screening multiple genes[3]. With the extensive use of high-throughput sequencing in prognosis research, various bioinformatics databases such as TCGA provide a useful data platform for constructing prediction models. However, considering that GC's therapeutic strategies are still limited, it is still necessary to develop new prognostic models.

Ferroptosis is a Fe-dependent, new kind about programmed cell demise. It is characterized by the increase of Fe-dependent lipid reactive oxygen species. Its concept was first introduced in 2012[4]. In subsequent studies, it was found that glutathione peroxidase 4(GPX4) mediated signaling pathway played an essential role in ferroptosis, and FSP1 was also found to play a similarly important role as GPX4 in

ferroptosis[5-6]. Further studies have revealed the regulation of cadherin-regulated intracellular interactions on ferroptosis[7].In cancer, ferroptosis may have cancer inhibiting function and can be used to treat cancer[8-9]. With the study revealing that CD8+T cells can regulate tumor cells' ferroptosis process through IFNγ[10], a link has been established between ferroptosis and tumor immunity. The correlation between GC and ferroptosis has been covered by some studies[11-14]. Several genes may be included for regulating ferroptosis in GC and influence the progression from GC, but the correlation with OS rate in GC patients has not been clarified.

ECM is an essential component of the tumor microenvironment, and its related characteristics and components play an important role in the proliferation, apoptosis, metabolism, and immune response of tumor cells[15]. In cancer, the remodeling of ECM and changes in the immune environment directly or indirectly affect tumor occurrence and development. Among them, macrophages[16-18], NK cells[19-20] and T cells[21-22] have been confirmed to guide the changes of the immune microenvironment through ECM, thereby affecting the tumor cells. In addition, as important components of ECM, collagen and fibroblasts are also involved in tumor immune changes[23-24].

This study downloaded mRNA expression profiles and relating clinical information of GC patients from a public database and obtained ferroptosis-related genes. A prognostic model with differentially expressed genes related to ferroptosis was constructed and verified. The potential mechanism was further explored through functional enrichment analysis. Finally, we identified 11 ferroptosis-related genes that affected GC's prognosis and established the risk scoring model.

Materials And Methods

Data download

The mRNA expression data (RNA-seq) of 407 patients with GC and clinical data were downloaded from the public database of TCGA (https://portal.gdc.cancer.gov/) updated on September 16, 2020. Data on 259 ferroptosis-related genes were obtained by downloading the FerrDb database (http://www.zhounan.org/ferrdb/).

Obtaining ferroptosis-related genes with prognostic value

Based on the FDR < 0.05, the downloaded TCGA data were standardized using the "Limma" R package in the R programming environment to obtain the DEGs between GC tissues and normal paracancerous tissues, and to extract the ferroptosis-related genes from the DEGs. The OS was determined by univariate COX analysis to screen genes with prognostic value. Then, in the R programming environment, the Venn diagram was drawn using the "Venn" R package, and the intersection genes of the DEGs and the prognostic genes were taken to obtain the ferroptosis-related genes with prognostic value. These genes were analyzed using the "pheatmap" and "survival" R packages to produce heat maps and forest maps.

Besides, the PPI network was obtained through the STRING database[25], and the correlation network was plotted using the "Igraph" R package.

Construct a prognosis model

The LASSO-penalized Cox regression analysis[26-27] was applied to chosen the genes related to survival and prognosis selected by univariate COX analysis to ensure the best fitting error and obtain the lowest variables risk of overfitting to improve the accuracy of the model. The penalty parameter(λ) of the model is obtained by the self-contained "cv.glmnet" function in the "glmnet" R package. With the expression matrix of the screened candidate prognostic DEGs as an independent variable and the overall survival time and status as the response variables, the multivariate COX analysis was carried out to construct the prognosis model. The risk score was computed in light of each gene's expression level and the corresponding correlation coefficient. Formula: risk score = $\sum$(expression level of each gene×correlation coefficient of that gene, coef). As stated by the median value of risk values, those patients were divided into high-risk and low-risk groups.

Survival analysis

The "Survminer" R package was used in the R programming environment to determine the optimal cut-off expression value, and the Kaplan-Meier survival curve was drawn by the "Survival" R package ($P<0.05$). The ROC curve was drawn by "SurvivalROC" R package, and the area under the AUC curve is used to evaluate the model's predictive value. Also, to investigate the distribution of diverse groups, the "stats" R package and "Rtsne" R packages were utilized to PCA and t-SNE analysis.

Functional enrichment analysis

The "clusterProfiler" R package was used for GO and KEGG analysis of DEGs. The ssGSEA[28] was used to score 16 immune cells' infiltration and calculate 13 immune-related pathways' activities.

Statistical analysis

Kaplan-Meier analysis was used to assess the OS between different groups. To determine independent predictors of OS, univariate and multivariate Cox regression analyses were used. Assess the relationship between clinical data and risk scores. The ssGSEA scores of immune cells or pathways among different groups were compared by Mann-Whitney test ($P < 0.05$). All relevant statistical analysis and mapping work was performed using the above R software (Version 4.0.2) and R packages.

Result

The flow of this study is shown in **Figure 1**. We downloaded what added up to 407 GC patients from the TCGA database, including 375 GC samples and 32 normal para-cancer samples. The detailed clinical features of these patients are shown in **Table 1**.

Acquisition of prognostic ferroptosis-related DEGs

What added up to 259 ferroptosis-related genes were extracted from the FerrDb database(**Figure 2a**). Among them, 170 genes showed significant expression differences between GC samples and normal para-cancer samples, and 18 prognostic genes were screened out by univariate COX regression analysis (FDR<0.05, **Figure 2**). The heat map and forest map of the 18 genes are shown in **figures 2b-c**. The PPI network of these 18 genes was constructed in the STRING database, and it was found that CAV1, DUSP1, SP1, and NOX4 were the critical genes in this PPI network (**Figure 2d**). In addition, the correlation network of the 18 genes is indicated done **Figure 2e**.

Construction and validation of the prognostic model

Those 18 prognostic ferroptosis-related genes were further screened by LASSO regression analysis. The optimal λ value was calculated, and the corresponding 11 genes with the most reduced cross-validation lapse were chosen (**figures 3a-b**). Finally, a model was constructed based on the 11 genes. The risk score has been computed dependent upon each gene's expression level and the corresponding correlation coefficient (coef) (**Table 2**), and the patients were partitioned under a high-risk group and a low-risk group with the risk values' median value. (**Figure 4a**). The survival prognosis of the low-risk group is higher than that of the high-risk group through the Kaplan-Meier survival curve analysis(p=1.651e-04) (**Figure 4b**). The area under the AUC curve in the ROC curve was used to evaluate the model's prediction reliability, and as shown in **Figure 4c**, the model had good sensitivity. PCA and t-SNE analyses showed that patients' distribution in the two risk groups was in two directions (**Figure 4d-e**). Besides, patients with high-risk died earlier than the low-risk group (**Figure 4f**).

Analysis of the independent prognostic value of the model

To determine whether the established prognosis model can be used as a prognostic factor independent of other clinical features, univariate and multivariate COX regression analysis was used for verification. The results showed a significant correlation between risk scores and OS in both univariate and multivariate Cox regression analyses (HR=3.627, 95% CI=2.256-5.829, p<0.001, **Figure 5a**; HR=4.176, 95% CI=2.588-6.736, P<0.001, **Figure 5b**). Previously summary, the risk score of the prognostic model we constructed can be used as an independent prognostic factor.

Function analysis of the prognosis model

GO and KEGG analyses of DEGs between the two risk groups were performed to dissect related biological functions and pathways. Those outcomes indicated that the DEGs were significantly enriched in extracellular matrix (ECM) related biological processes, including ECM organization, collagen-containing ECM, focal adhesion, ECM structural constituent, collagen binding, ECM binding (P. adjust<0.05, **Figure 6a**). KEGG pathway analysis showed that these DEGs were also enriched in ECM related pathways, such as proteoglycans in cancer and ECM-receptor interactions (P. adjust<0.05, **Figure 6b**). Besides, these DEGs are enriched in the muscle system.

Tumor-targeted immunotherapy is a hot topic nowadays. ECM has been speculated as a part of health and homeostasis, plays a critical immunomodulatory role[29], and the synergistic antitumor effect between ECM and the immune system will be the focus of future research.

Therefore, ssGSEA is used to quantify the enrichment scores of different immune cell subsets, related functions, or pathways further to explore the correlation between risk scores and immune status. The results showed significant differences in mast cells, neutrophils, T helper cells, and Th2 cells between these two different risk groups (P. adjust<0.05, **Figure 7a**). In the KEGG analysis, except for the fact that MHC class I had a lower score in the low-risk group, others including APC co-stimulation, cytokine-cytokine receptor interaction (CCR), type IFN response, parainflammation, and type IFN response were all scored higher in the high-risk group (P. adjust<0.05, Figure 7b).

Discussion

In the present study, we analyzed 259 ferroptosis-related genes in GC tissues and their relationship with OS. More than a large portion of the ferroptosis-related genes (65. 6%) were differentially expressed in GC tissues and adjacent non-tumor tissues. Also, 18 genes are associated with OS, which also indicates, to some extent, the possibility part of ferroptosis in GC. Therefore, we then constructed a new prognostic model containing 11 ferroptosis-related genes and further validated the prognostic model.

The prognostic model constructed in this study included 11 ferroptosis-related genes (NOX4, NOX5, SLC1A5, GLS2, MYB, TGFBR1, NF2, ZFP36, DUSP1, SLC1A4, SP1). NOX4 can catalyze the molecular oxidation-reduction to reactive oxygen species (ROC). Also, ROC assumes a crucial part in the ferroptosis[30]. In melanoma, miR-137 can negatively regulate cells' ferroptosis by directly targeting the glutamine transporter SLC1A5[31]. GLS2 is an essential transporter of glutamine to glutamic acid. In GC, physcion8-O-β-glucopyranoside (PG) plays a Fe-promoting and anti-tumor role in vivo and vitro by regulating the miR-103a-3p/GLS2 axis[13]. One of the characteristics of ferroptosis is the loss of GPX4 activity. Studies have shown that c-Myb transcription regulates cysteine dioxygenase 1(CDO1) and up-regulates the expression of GPX4 by inhibiting the expression of CDO1[11]. Ferroptosis can be regulated by non-cell-autonomously through cadherin-mediated intercellular interactions, mediated by the activation of intracellular NF2 and Hippo signaling pathways, thereby inhibiting ferroptosis[7]. In the study of intestinal ischemia-reperfusion injury, inhibition of ACSL4 before reperfusion protects the process of ferroptosis, during which Sp1 can serve as a critical transcription factor that binds to the ACSL4 promoter region and improves the transcription of ACSL4[32]. To sum up, in the prognostic model we constructed, the six genes(NOX4, SLC1A5, GLS2, MYB, NF2, and SP1) have been confirmed to participate in the process of ferroptosis, while the five genes (NOX5, SLC1A4, TGFBR1, ZFP36, and DUSP1) have not been confirmed to be related to ferroptosis. In conclusion, these 11 genes have been affirmed to be related to poor prognosis in our prognostic model. Nevertheless, whether these genes affect the prognosis of patients with GC through the process related to ferroptosis has not been studied in depth. GLS2 alone has been studied for the correlation between GC and ferroptosis. In our GO and KEGG analysis results, the

enrichment areas of biological processes and pathways are in the extracellular matrix. The research by Brown et al.[33] proposed that ECM separation of cells lacking GPX4 was the physiological trigger for ferroptosis. Studies have shown that in tumors, porcine bladder ECM has anti-tumor cell activity, and this function is not directly acting on tumor cells but mediated by immune cells[34]. Badylak[29] explored the future research prospect between ECM and tumor immunity and speculated that the presence of individual-specific signaling molecules in ECM would cause the anti-tumor phenotype of immune cells them possess anti-tumor cell activity. In the further immune-related analysis, many immune cells and immune-related functional pathways were found to be statistically different, which also provides a theoretical basis for us to speculate that ferroptosis may be potentially related to tumor immunity. However, the current study on the potential relationship between tumor immunity and ferroptosis is still preliminary. The proportion of mast cells and neutrophils was higher in the high-risk group. Mast cells exist as immune cells in almost all vascularized tissues, and in tumors, they can affect tumor development, tumor tissue angiogenesis, and the adaptive immune response of tumors[35]. The increase in mast cell density in GC is accompanied by an increase in the release of related angiogenic and lymphangiogenic factors to promote tumor cells' proliferation[36]. Neutrophils are well known in infections of the organism. In tumors, tumor-associated neutrophils can induce angiogenesis, ECM remodeling, metastasis, and immunosuppression[37]. The function of these immune cells in the tumor microenvironment allows us to speculate whether the cells release special signals during the ferroptosis, so that mast cells and neutrophils promote angiogenesis and further promote the proliferation metastasis of tumor cells. Besides, we found noteworthy contrasts in the antigen presentation procedure between those two risk groups, with a higher risk score associated with impaired anti-tumor immunity, including the activity of type I and type II IFN responses. It has been speculated that antigen-presenting cells (APCs) are attracted to dead cells' sites during the ferroptosis[38]. Study has found that cancer cells that induce the death of immunogenic cancer cells (ICD) can coordinate "change self-mimicry" at the level of nucleic acid or chemokine, leading to type I IFN response[39]. In conclusion, the changes in the immune environment and weakened anti-tumor immune function in the high-risk group of GC patients may lead to poor prognosis of GC patients.

This study successfully constructed a prognostic model for GC and verified its reliability, but this model's data were retrospective. Besides, due to public databases' limitation, we did not use data from multiple public databases to further verify the constructed model. Finally, the link between the risk score in the model and the ECM as well as the immune system has not been experimentally verified.

Conclusions

This study investigates 11 ferroptosis-related genes(NOX4, NOX5, SLC1A5, GLS2, MYB, TGFBR1, NF2, ZFP36, DUSP1, SLC1A4, SP1) were identified, and a new prognostic model for GC was constructed. The model has been further confirmed to be capable of predicting the prognosis of patients with GC and has provided a potential new research direction for predicting GC's prognosis. Besides, the potential

relationship between these genes and ECM as well as tumor immunity is also the subject of further research in the future.

Abbreviations

GC: Gastric cancer; ECM: Extracellular matrix; OS: Overall survival; TCGA: The Cancer Genome Atlas; GO: Gene ontology; KEGG: Kyoto Encyclopedia of Genes and Genomes; ssGSEA: Single-sample gene set enrichment analysis; FerrDb: Database of ferroptosis; DEGs: Differentially expressed genes; LASSO: Least absolute shrinkage and selection operator; Coef: Correlation coefficient of the gene; ROC: Receiver operating characteristic; FDR: False discovery rate; PCA: Principal component analysis; t-SNE: t-distributed stochastic neighbor embedding; AUC: Area under the curve; HR: Hazard ratio; CI: Confidence interval; APC: Antigen presenting cell; CCR: Cytokine-cytokine receptor; ICD: immunogenic cancer cells.

Declarations

Ethics approval and consent to participate

There were no cell, tissue, or animal studies. No ethical requirements are involved.

Consent for publication

All authors agree to publish the paper.

Availability of data and materials

The data used to support the findings of this study are included within the article.

Competing interests

The authors declare that they have no competing interests.

Funding

This work was supported by grants from the National Natural Science Foundation of China (No. 81602425), the Natural Science Foundation of Anhui Province (No. 1508085QH152).

Authors' contributions

Bang Chen is responsible for writing and submitting the papers; Xin Xu, ShaoFu Zhu, and ShiYi Yang are responsible for data analysis and collation; Kang Yang, MengYao Jin, Tianbin Wang, and Tao Men are responsible for the production of pictures;Guodong Cao and Bo Chen is responsible for the manuscript fees and ideas guidance. The authors read and approved the final manuscript.

Acknowledgements

We acknowledge the support received from the National Natural Science Foundation of China (No. 81602425) and the Natural Science Foundation of Anhui Province (No. 1508085QH152).

References

1. Bray F, Ferlay J, Soerjomataram I, Siegel RL, Torre LA, Jemal A. Global cancer statistics 2018: GLOBOCAN estimates of incidence and mortality worldwide for 36 cancers in 185 countries. CA Cancer J Clin. 2018;68(6):394–424.
2. Chen W, Zheng R, Baade PD, Zhang S, Zeng H, Bray F, Jemal A, Yu XQ, He J. Cancer statistics in China, 2015. CA Cancer J Clin. 2016;66(2):115-32.
3. Jiang K, Liu H, Xie D, Xiao Q. Differentially expressed genes ASPN, COL1A1, FN1, VCAN and MUC5AC are potential prognostic biomarkers for gastric cancer. Oncol Lett. 2019;17(3):3191-202.
4. Dixon SJ, Lemberg KM, Lamprecht MR, Skouta R, Zaitsev EM, Gleason CE, Patel DN, Bauer AJ, Cantley AM, Yang WS, Morrison B 3rd, Stockwell BR. Ferroptosis: an iron-dependent form of nonapoptotic cell death. Cell. 2012;149(5):1060-72.
5. Bersuker K, Hendricks JM, Li Z, Magtanong L, Ford B, Tang PH, Roberts MA, Tong B, Maimone TJ, Zoncu R, Bassik MC, Nomura DK, Dixon SJ, Olzmann JA. The CoQ oxidoreductase FSP1 acts parallel to GPX4 to inhibit ferroptosis. Nature. 2019;575(7784):688-92.
6. Doll S, Freitas FP, Shah R, Aldrovandi M, da Silva MC, Ingold I, Goya Grocin A, Xavier da Silva TN, Panzilius E, Scheel CH, Mourão A, Buday K, Sato M, Wanninger J, Vignane T, Mohana V, Rehberg M, Flatley A, Schepers A, Kurz A, White D, Sauer M, Sattler M, Tate EW, Schmitz W, Schulze A, O'Donnell V, Proneth B, Popowicz GM, Pratt DA, Angeli JPF, Conrad M. FSP1 is a glutathione-independent ferroptosis suppressor. Nature. 2019;575(7784):693-8.
7. Wu J, Minikes AM, Gao M, Bian H, Li Y, Stockwell BR, Chen ZN, Jiang X. Intercellular interaction dictates cancer cell ferroptosis via NF2-YAP signalling. Nature. 2019;572(7769):402-6.
8. Stockwell BR, Friedmann Angeli JP, Bayir H, Bush AI, Conrad M, Dixon SJ, Fulda S, Gascón S, Hatzios SK, Kagan VE, Noel K, Jiang X, Linkermann A, Murphy ME, Overholtzer M, Oyagi A, Pagnussat GC, Park J, Ran Q, Rosenfeld CS, Salnikow K, Tang D, Torti FM, Torti SV, Toyokuni S, Woerpel KA, Zhang DD. Ferroptosis: A Regulated Cell Death Nexus Linking Metabolism, Redox Biology, and Disease. Cell. 2017;171(2):273-85.
9. Hassannia B, Vandenabeele P, Vanden Berghe T. Targeting Ferroptosis to Iron Out Cancer. Cancer Cell. 2019 ;35(6):830-49.
10. Wang W, Green M, Choi JE, Gijón M, Kennedy PD, Johnson JK, Liao P, Lang X, Kryczek I, Sell A, Xia H, Zhou J, Li G, Li J, Li W, Wei S, Vatan L, Zhang H, Szeliga W, Gu W, Liu R, Lawrence TS, Lamb C, Tanno Y, Cieslik M, Stone E, Georgiou G, Chan TA, Chinnaiyan A, Zou W. CD8+ T cells regulate tumour ferroptosis during cancer immunotherapy. Nature. 2019;569(7755):270-4.

11. Hao S, Yu J, He W, Huang Q, Zhao Y, Liang B, Zhang S, Wen Z, Dong S, Rao J, Liao W, Shi M. Cysteine Dioxygenase 1 Mediates Erastin-Induced Ferroptosis in Human Gastric Cancer Cells. Neoplasia. 2017;19(12):1022-32.
12. Asghar W, El Assal R, Shafiee H, Pitteri S, Paulmurugan R, Demirci U. Engineering cancer microenvironments for in vitro 3-D tumor models. Mater Today (Kidlington). 2015;18(10):539-53.
13. Shimizu-Hirota R, Xiong W, Baxter BT, Kunkel SL, Maillard I, Chen XW, Sabeh F, Liu R, Li XY, Weiss SJ. MT1-MMP regulates the PI3Kδ·Mi-2/NuRD-dependent control of macrophage immune function. Genes Dev. 2012 Feb 15;26(4):395-413. doi: 10.1101/gad.178749.111. Erratum in: Genes Dev. 2012;26(10):1122.
14. Alonso-Nocelo M, Raimondo TM, Vining KH, López-López R, de la Fuente M, Mooney DJ. Matrix stiffness and tumor-associated macrophages modulate epithelial to mesenchymal transition of human adenocarcinoma cells. Biofabrication. 2018;10(3):035004.
15. Larsen AMH, Kuczek DE, Kalvisa A, Siersbæk MS, Thorseth ML, Johansen AZ, Carretta M, Grøntved L, Vang O, Madsen DH. Collagen Density Modulates the Immunosuppressive Functions of Macrophages. J Immunol. 2020;205(5):1461-72.
16. Brennan TV, Lin L, Brandstadter JD, Rendell VR, Dredge K, Huang X, Yang Y. Heparan sulfate mimetic PG545-mediated antilymphoma effects require TLR9-dependent NK cell activation. J Clin Invest. 2016;126(1):207-19.
17. Xu Y, Pang SW. Natural killer cell migration control in microchannels by perturbations and topography. Lab Chip. 2019 Jul 21;19(14):2466-75.
18. Jensen C, Madsen DH, Hansen M, Schmidt H, Svane IM, Karsdal MA, Willumsen N. Non-invasive biomarkers derived from the extracellular matrix associate with response to immune checkpoint blockade (anti-CTLA-4) in metastatic melanoma patients. J Immunother Cancer. 2018;6(1):152.
19. Kuczek DE, Larsen AMH, Thorseth ML, Carretta M, Kalvisa A, Siersbæk MS, Simões AMC, Roslind A, Engelholm LH, Noessner E, Donia M, Svane IM, Straten PT, Grøntved L, Madsen DH. Collagen density regulates the activity of tumor-infiltrating T cells. J Immunother Cancer. 2019;7(1):68.
20. Kalluri R. The biology and function of fibroblasts in cancer. Nat Rev Cancer. 2016;16(9):582-98.
21. Jürgensen HJ, van Putten S, Nørregaard KS, Bugge TH, Engelholm LH, Behrendt N, Madsen DH. Cellular uptake of collagens and implications for immune cell regulation in disease. Cell Mol Life Sci. 2020;77(16):3161-76.
22. Li C, Tian Y, Liang Y, Li Q. Circ_0008035 contributes to cell proliferation and inhibits apoptosis and ferroptosis in gastric cancer via miR-599/EIF4A1 axis. Cancer Cell Int. 2020 Mar 16;20:84.
23. Niu Y, Zhang J, Tong Y, Li J, Liu B. Physcion 8-O-β-glucopyranoside induced ferroptosis via regulating miR-103a-3p/GLS2 axis in gastric cancer. Life Sci. 2019;237:116893.
24. Zhang H, Deng T, Liu R, Ning T, Yang H, Liu D, Zhang Q, Lin D, Ge S, Bai M, Wang X, Zhang L, Li H, Yang Y, Ji Z, Wang H, Ying G, Ba Y. CAF secreted miR-522 suppresses ferroptosis and promotes acquired chemo-resistance in gastric cancer. Mol Cancer. 2020;19(1):43.

25. Szklarczyk D, Franceschini A, Kuhn M, Simonovic M, Roth A, Minguez P, Doerks T, Stark M, Muller J, Bork P, Jensen LJ, von Mering C. The STRING database in 2011: functional interaction networks of proteins, globally integrated and scored. Nucleic Acids Res. 2011 Jan;39(Database issue):D561-8.
26. Simon N, Friedman J, Hastie T, Tibshirani R. Regularization Paths for Cox's Proportional Hazards Model via Coordinate Descent. J Stat Softw. 2011;39(5):1-13.
27. Tibshirani R. The lasso method for variable selection in the Cox model. Stat Med. 1997;16(4):385-95.
28. Rooney MS, Shukla SA, Wu CJ, Getz G, Hacohen N. Molecular and genetic properties of tumors associated with local immune cytolytic activity. Cell. 2015;160(1-2):48-61.
29. Badylak SF. Extracellular matrix and the immune system: friends or foes. Nat Rev Urol. 2019;16(7):389-90.
30. Yang WH, Ding CC, Sun T, Rupprecht G, Lin CC, Hsu D, Chi JT. The Hippo Pathway Effector TAZ Regulates Ferroptosis in Renal Cell Carcinoma. Cell Rep. 2019;28(10):2501-8.
31. Luo M, Wu L, Zhang K, Wang H, Zhang T, Gutierrez L, O'Connell D, Zhang P, Li Y, Gao T, Ren W, Yang Y. miR-137 regulates ferroptosis by targeting glutamine transporter SLC1A5 in melanoma. Cell Death Differ. 2018;25(8):1457-72.
32. Li Y, Feng D, Wang Z, Zhao Y, Sun R, Tian D, Liu D, Zhang F, Ning S, Yao J, Tian X. Ischemia-induced ACSL4 activation contributes to ferroptosis-mediated tissue injury in intestinal ischemia/reperfusion. Cell Death Differ. 2019;26(11):2284-99.
33. Brown CW, Amante JJ, Goel HL, Mercurio AM. The α6β4 integrin promotes resistance to ferroptosis. J Cell Biol. 2017;216(12):4287-97.
34. Wolf MT, Ganguly S, Wang TL, Anderson CW, Sadtler K, Narain R, Cherry C, Parrillo AJ, Park BV, Wang G, Pan F, Sukumar S, Pardoll DM, Elisseeff JH. A biologic scaffold-associated type 2 immune microenvironment inhibits tumor formation and synergizes with checkpoint immunotherapy. Sci Transl Med. 2019;11(477):7973.
35. Marichal T, Tsai M, Galli SJ. Mast cells: potential positive and negative roles in tumor biology. Cancer Immunol Res. 2013;1(5):269-79.
36. Sammarco G, Varricchi G, Ferraro V, Ammendola M, De Fazio M, Altomare DF, Luposella M, Maltese L, Currò G, Marone G, Ranieri G, Memeo R. Mast Cells, Angiogenesis and Lymphangiogenesis in Human Gastric Cancer. Int J Mol Sci. 2019;20(9):2106.
37. Jaillon S, Ponzetta A, Di Mitri D, Santoni A, Bonecchi R, Mantovani A. Neutrophil diversity and plasticity in tumour progression and therapy. Nat Rev Cancer. 2020;20(9):485-503.
38. Friedmann Angeli JP, Krysko DV, Conrad M. Ferroptosis at the crossroads of cancer-acquired drug resistance and immune evasion. Nat Rev Cancer. 2019;19(7):405-14.
39. Garg AD, Agostinis P. Cell death and immunity in cancer: From danger signals to mimicry of pathogen defense responses. Immunol Rev. 2017;280(1):126-48.

Tables

Table1 Clinical data of the GC patients in the present study			
Clinical information	**Number**	**%**	**Dead number**
All patients	443		
Age			
<65	185	41.8%	63
≧65	253	57.1%	108
unknow	5	1.1%	0
Gender			
Male	285	64.3%	114
Female	158	35.7%	57
Grade			
G1	12	2.7%	3
G2	159	35.9%	56
G3	263	59.4%	108
unknow	9	2.0%	4
Stage			
Stage I-II	189	42.7%	49
Stage III-IV	227	51.2%	111
unknow	27	6.1%	11
T			
T1-2	116	26.2%	31
T3-4	317	71.6%	135
unknow	10	2.2%	5
M			
M0	391	88.3%	146
M1	30	6.8%	17
unknow	22	4.9%	8
N			
N0	132	29.8%	32

N1-3	292	65.9%	134
unknow	19	4.3%	5

Table 2 The 11 genes that construct the model and their corresponding correlation coefficients

Gene Symbol	Offificial Full Name	coef
NOX4	NADPH oxidase 4	0.435186800403704
NOX5	NADPH oxidase 5	1.39826069008869
SLC1A5	solute carrier family 1 member 5	-0.0100869968303555
GLS2	glutaminase 2	-0.182243865540611
MYB	MYB proto-oncogene, transcription factor	-0.056027672741676
TGFBR1	transforming growth factor beta receptor 1	0.0573492611306872
NF2	neurofibromin 2	-0.216489649659101
ZFP36	Zinc finger protein 36	0.0676432596756568
DUSP1	dual specificity phosphatase 1	0.0165355623061305
SLC1A4	solute carrier family 1 member 4	-0.101454970676693
SP1	Sp1 transcription factor	-0.0983827137340583

Figures

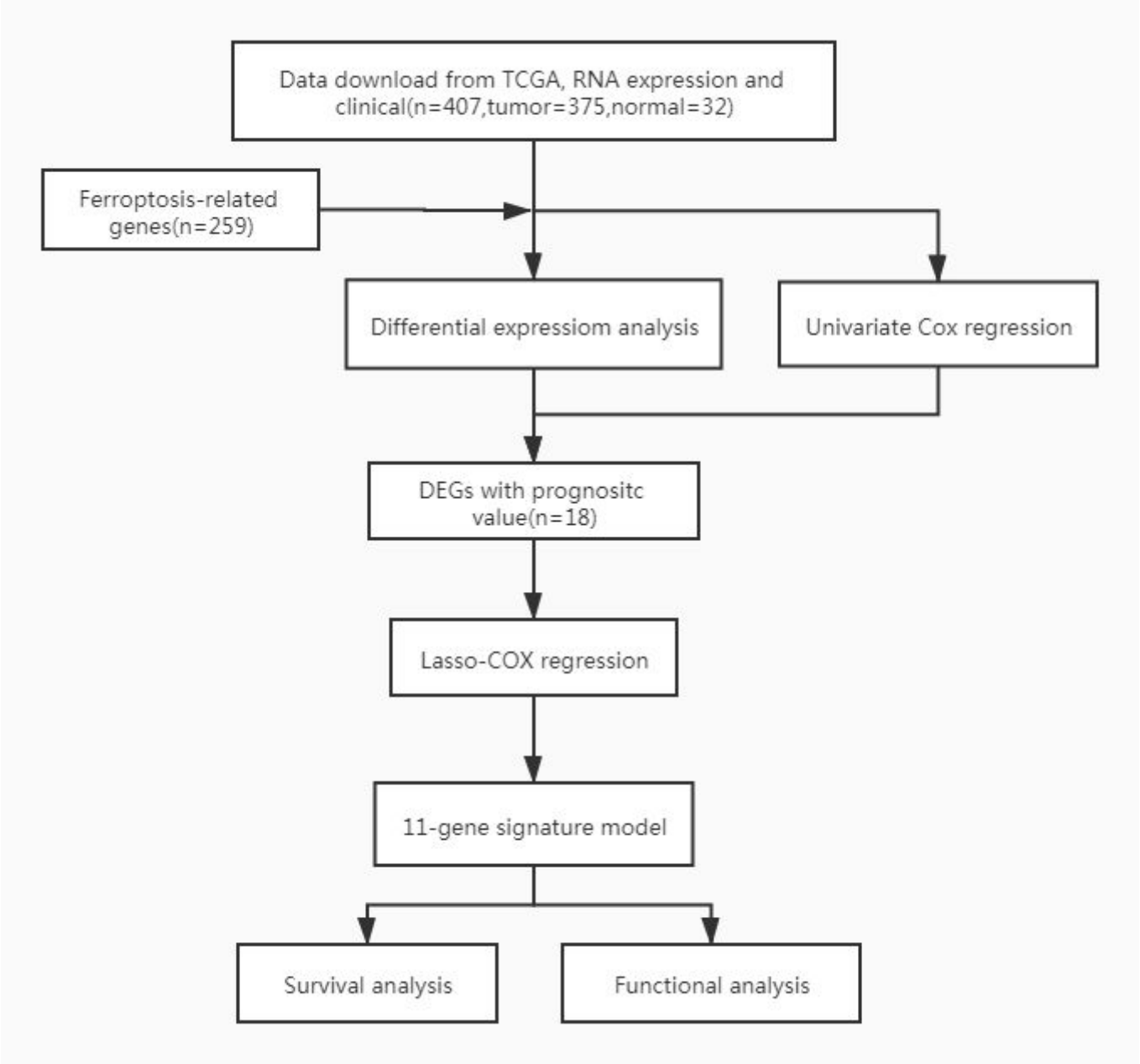

Figure 1

Flow chart of this study

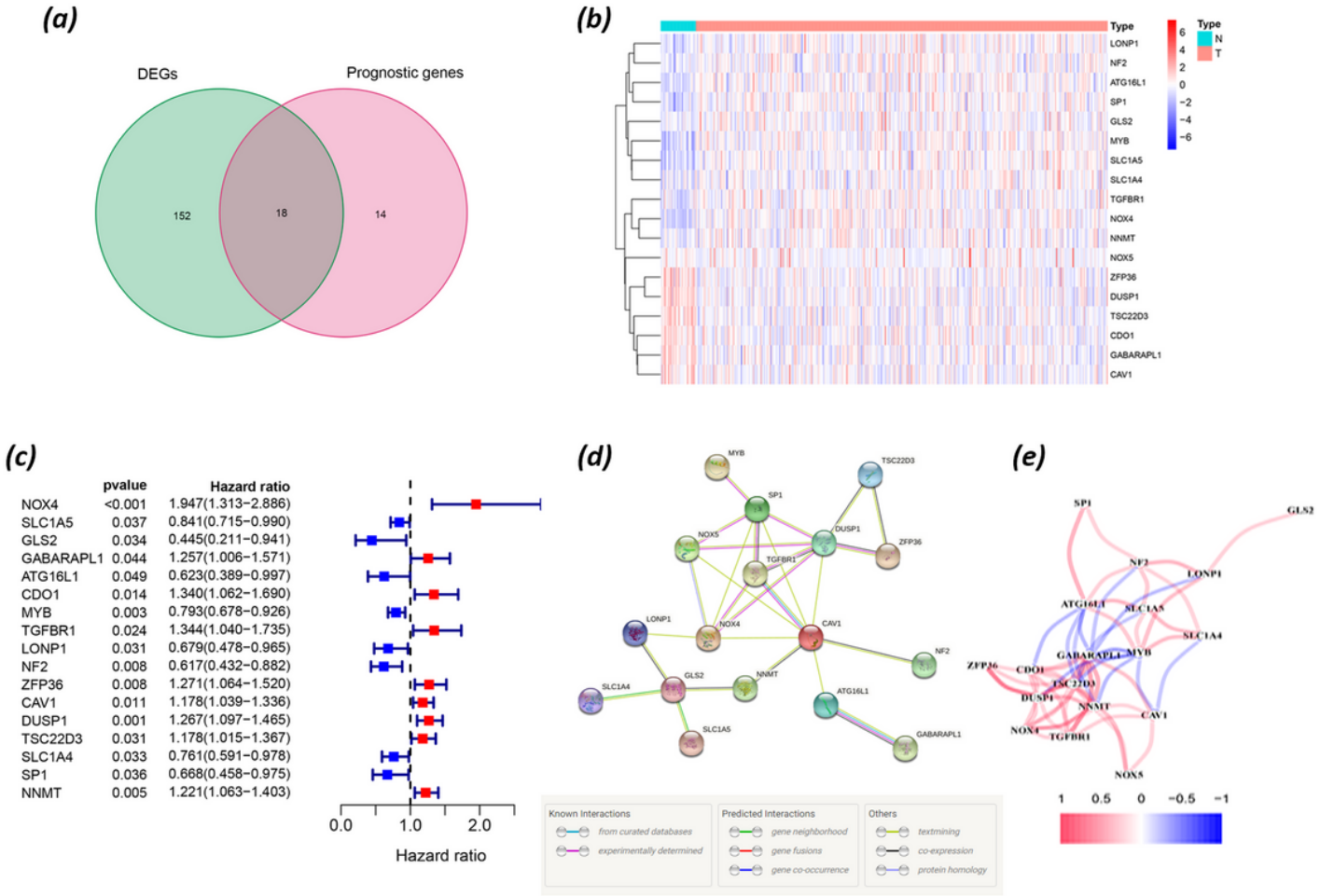

Figure 2

Identification of ferroptosis-related genes associated with prognosis. a. Venn diagram: 18 genes related to prognosis and differentially expressed in GC tissues and normal paracancerous tissues were screened out. b. expression of 18 candidate genes in tumor tissue and normal paracancerous tissue. c. forest plots: the relationship between gene expression and OS was shown by univariate Cox regression analysis. d. the PPI network of 18 candidate genes. e. the correlation network of 18 candidate genes.

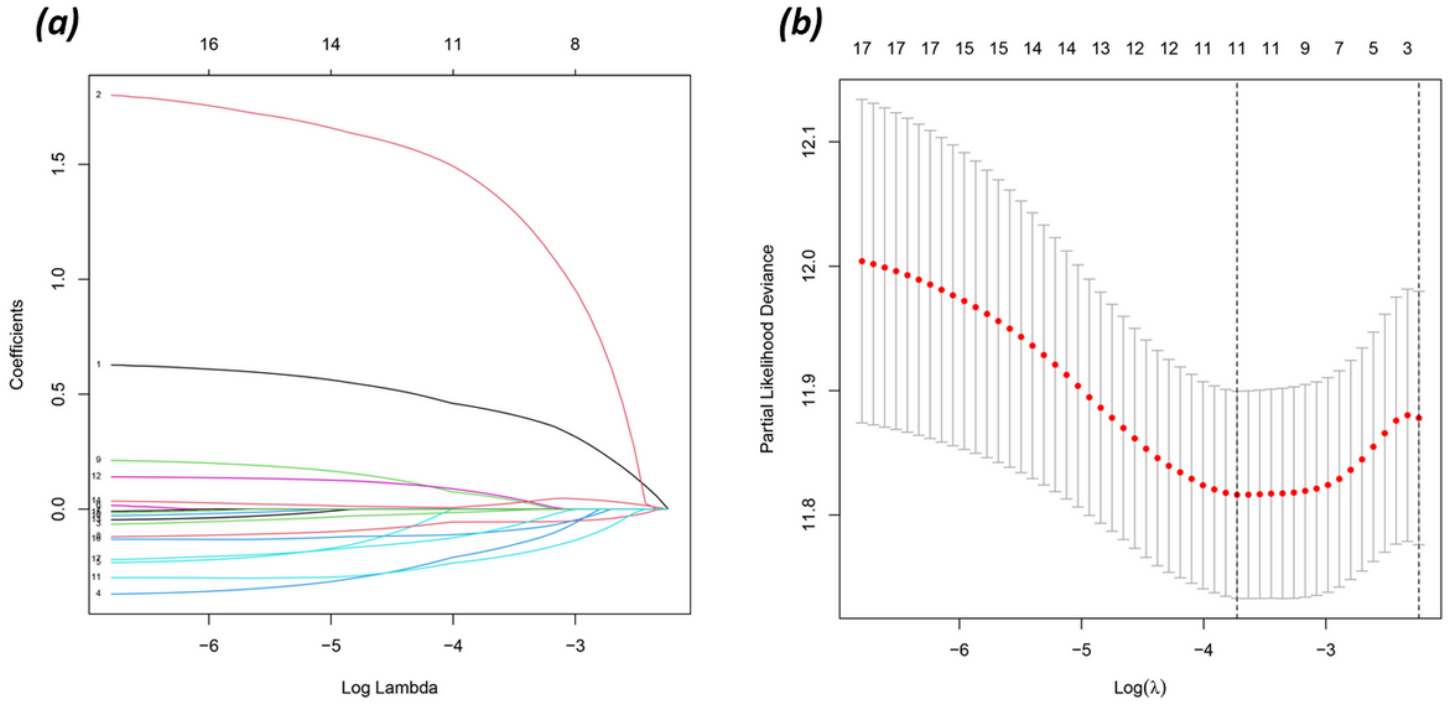

Figure 3

Through lasso regression analysis, 11 ferroptosis-related genes were identified to construct the prognosis model. a. LASSO coefficient of 18 candidate genes. b. determine the penalty parameter (λ) in the model, and the dashed vertical line is drawn at the optimal value of the fitting error.

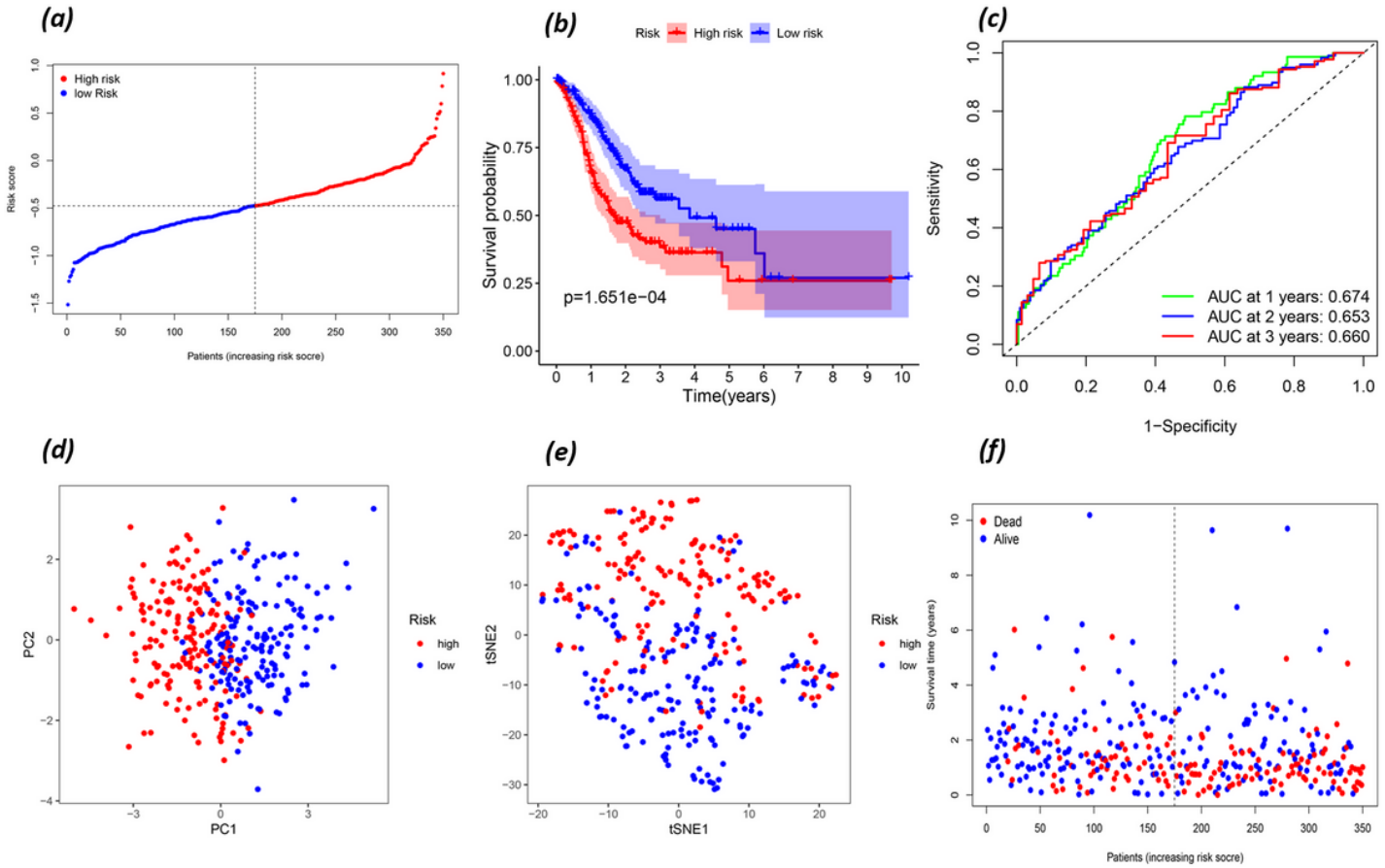

Figure 4

Prognostic analysis of a model constructed from 11 candidate genes. a. distribution and the median value of risk scores. b. Kaplan-Meier survival curves for patients in the high-risk and low-risk groups. c. ROC curve of the model, where AUC verifies that the sensitivity of the model is acceptable. d. PCA plot of the model. e. t-SNE analysis of the model. f. distribution of OS status and risk scores.

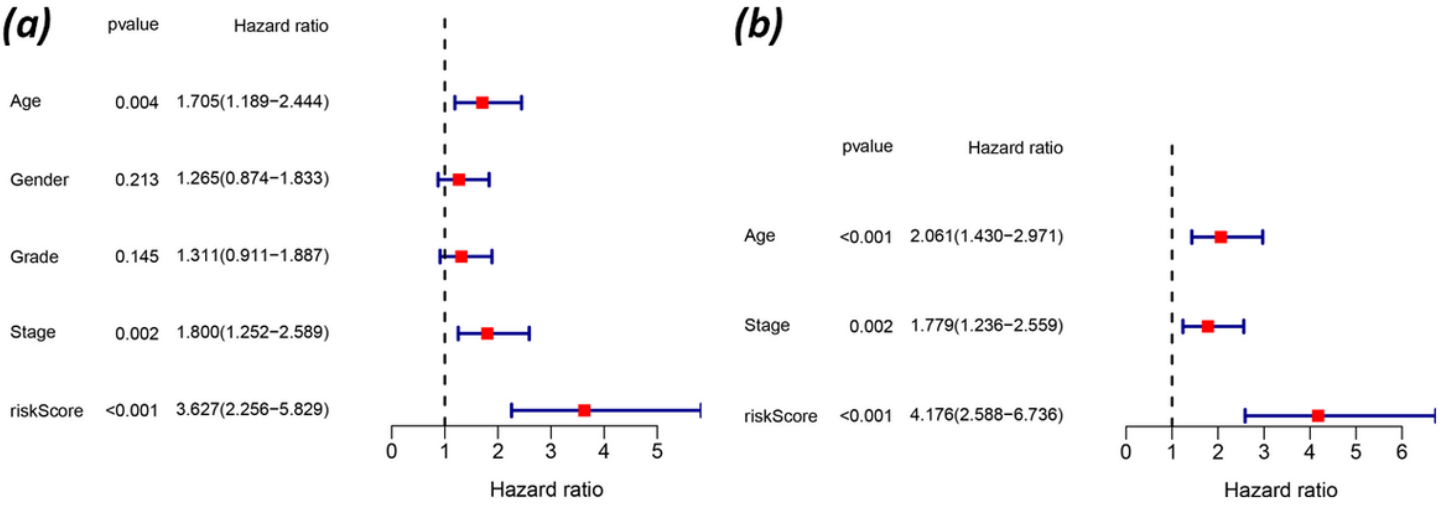

Figure 5

Results of univariate(a) and multivariate(b) Cox regression analysis for OS.

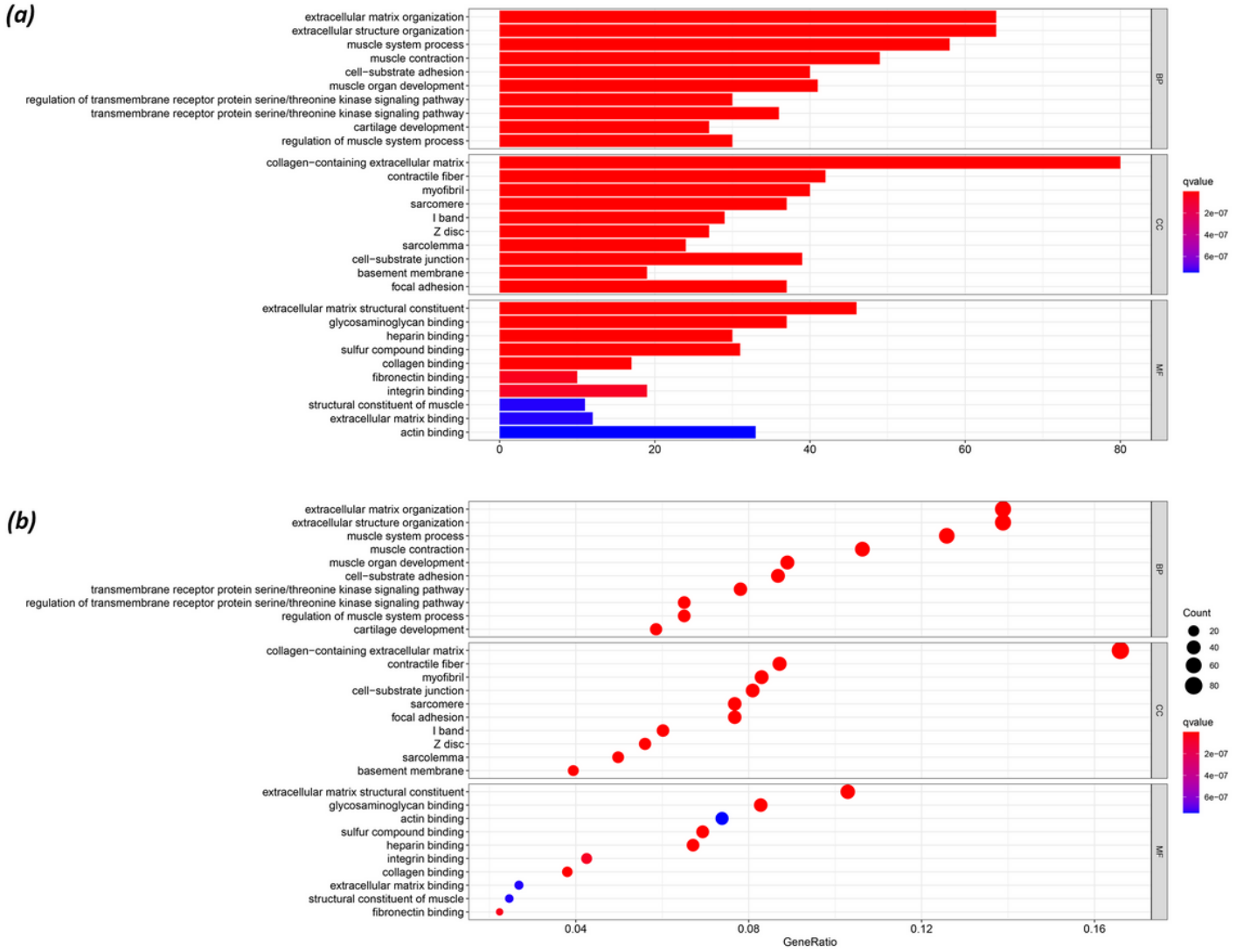

Figure 6

GO analysis of the prognostic model.

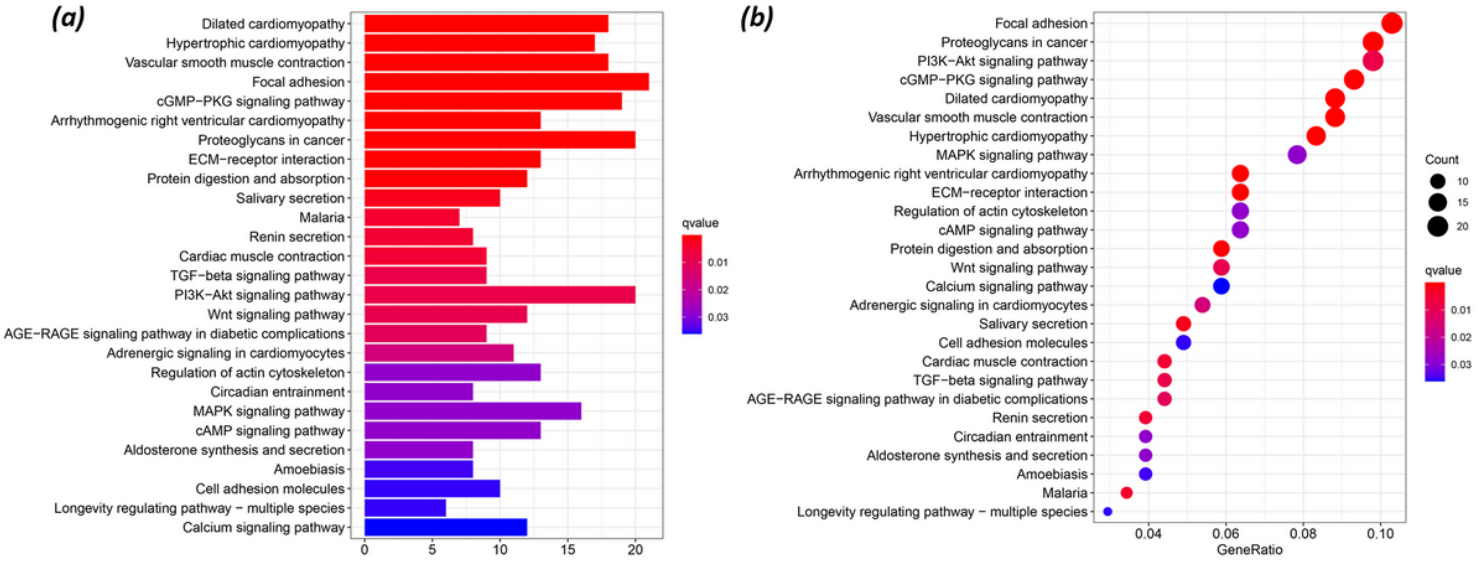

Figure 7

KEGG analysis of the prognostic model.

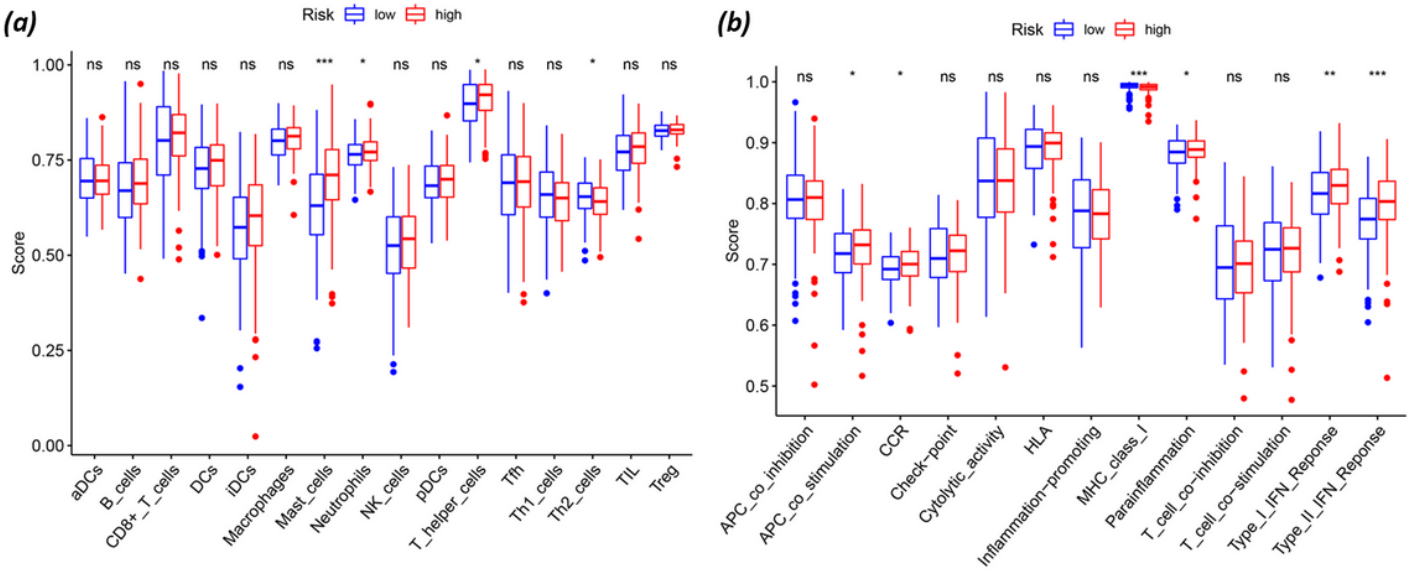

Figure 8

The ssGSEA scores of different risk groups were compared. a. Scores for 16 immune cells. b. Scores for 13 immune-related functions. (The adjusted P value was shown as ns, not significant; *, P < 0.05; **, P < 0.01; ***, P< 0.001.)